Journal of Physics: Conference Series **503** (2014) 012013 doi:10.1088/1742-6596/503/1/012013

Antihyperon-hyperon production in antiproton-proton annihilations with PANDA

Karin Schönning[a] and Erik Thomé[a] for the PANDA collaboration

[a] Dept. of Physics and Astronomy,bUppsala University, Box 516, 75120 Uppsala, Sweden

E-mail: karin.schonning@physics.uu.se

Abstract. Hyperon production is an excellent probe of the strong interaction in the confinement domain. The spin observables provide a powerful tool in understanding the underlying physical processes. Expressions of the seven non-zero polarisation parameters of the Ω baryon from decay angular distributions have recently been derived by the Uppsala group. Simulation studies show that all strange and single charmed hyperon production channels have great prospects with the PANDA detector.

1. Introduction

Hyperon production in $\overline{p}p \to \overline{Y}Y$ reaction gives important insights into strangeness and charm production. In this work, we consider single- and multi-strange and single-charmed hyperons. Their production from light-quark systems like $\overline{p}p$ implies processes where light quarks are replaced by heavier quarks. The relevant degrees of freedom of a certain process are given by its energy scale, which for strangeness production is governed by the mass of the strange quark, $m_s \approx 100$ MeV. This is close to the QCD cut-off, $\Lambda_{QCD} \approx 200$ MeV where the strong coupling constant, α_s, grows so large that perturbative QCD breaks down. As a consequence, it is unclear what the relevant degrees of freedom for processes involving strangeness production are: quarks and gluons, or hadrons? The production of strange hyperons therefore probes QCD in the intermediate region between the perturbative and the non-perturbative regime, *i.e.* the confinement domain, that we, up to now, know very little about. The scale of charm production is governed by $m_c \approx 1300$ MeV, more than ten times larger than m_s. The strong coupling constant in this region is $\alpha_s \approx 0.3$, just barely enough for a perturbative treatment to be valid. Comparing the production of strange hyperons with charmed could thus give important insights into the differences in the underlying physics at these two separate energy scales. Theoretical models describing hyperon production in $\overline{p}p \to \overline{Y}Y$ reactions are often based on the quark-gluon picture, where a light quark-antiquark pair from the initial nucleons annihilate into a gluon that splits into a heavier quark-antiquark pair ($s\overline{s}$ or $c\overline{c}$) [1]. For strange hyperons, there are also kaon exchange models, where the production of single (multiple) strangeness hyperons are modeled by the single (multiple) exchange of a t-channel kaon [2]. There have also been attempts to combine a quark-gluon approach with a kaon exchange approach [3].

Spin variables are often very powerful in discriminating between different theoretical models. The hyperon spin variables can be related to the spin of individual quarks. The Λ hyperon can be modeled by a ud spin 0 di-quark combined with an s-quark that carries the spin of the entire hyperon. A similar picture can be drawn for the Λ_c hyperon, and by comparing spin observables of Λ and Λ_c, we can learn about the role of spin in the creation of s- and c-quarks.

Another interesting aspect of hyperons is CP violation. One of the unsolved mysteries of contemporary physics is why the universe consists of matter while antimatter is almost absent. Violation of CP symmetry is one possible source that gives rise to this asymmetry [4]. CP violation has been observed in meson decays, but so far never for baryons. For hyperons, CP violation observables are accessible *via* angular distributions of hyperon decay products.

In this work, the potential of spin measurements in multi-strange and charmed hyperon production is described. First, we outline the polarisation parameters of spin $\frac{1}{2}$ and spin $\frac{3}{2}$ hyperons, the latter as recently derived by the Uppsala group. Then we present the spin observables of the full $\bar{p}p \to \overline{Y}Y$ process in the case of spin $\frac{1}{2}$ hyperons, based on previous work by *e.g* the PS185 collaboration. We conclude with the prospects for hyperon studies with PANDA, based on simulation studies performed by the Uppsala group.

2. Spin observables for spin $\frac{1}{2}$ and spin $\frac{3}{2}$ hyperons

Polarisation parameters for spin $\frac{1}{2}$ hyperons

All physics information about a quantum mechanical ensemble is contained within the density matrix ρ. In an expansion of hermitian matrices Q^L_M and polarisation parameters r^L_M [5], the density matrix of a particle of arbitrary spin j is given by

$$\rho = \frac{1}{2j+1} I + \sum_{L=1}^{2j} \frac{2j}{2j+1} \sum_{M=-L}^{L} Q^L_M r^L_M \tag{1}$$

where the first term denotes the unpolarised differential cross section I and the second the polarised part, containing the r^L_M parameters. L is the angular momentum and M its projection. In the case of spin $\frac{1}{2}$ particles, the Q^L_M are the Pauli matrices and the polarisation parameters correspond to the vector polarisations P_l, P_m and P_n. The indices are defined in the coordinate system in the left panel of Fig. 1. For particles produced in parity conserving processes, *e.g* hyperons in strong interactions, symmetries of the spin density matrix imply that $P_l = P_m = 0$, giving non-zero polarisation only perpendicular to the production plane. The angular distribution of a particle from a given decay can be expressed in terms of the spin density matrix of the mother particle: $I = T\rho_{initial}T^\dagger$, where T is the decay matrix [6]. For the case of a weak decay of a spin $\frac{1}{2}$ baryon into a spin $\frac{1}{2}$ baryon and a pseudoscalar meson, the final state can have angular momentum $L = 0$, that violates parity, or $L = 1$, that conserves parity. This gives a decay matrix with one parity violating part T_s and one parity conserving part T_p. From their products, the asymmetry parameters $\alpha = 2Re(T_s^* T_p)$, $\beta = 2Im(T_s^* T_p)$ and $\gamma = |T_s|^2 - |T_p|^2$ can be defined. By definition, they fulfill $\alpha^2 + \beta^2 + \gamma^2 = |T_s|^2 + |T_p|^2 = 1$. For example, in the $\Lambda \to p\pi^-$ decay, the angular distribution of the proton is given by

$$I(\cos\theta_p) = \frac{1}{4\pi}(1 + \alpha_\Lambda P_n \cos\theta_p). \tag{2}$$

Some hyperons decay into other hyperons, *e.g.* the Ξ baryons, as illustrated in the right panel of Fig. 1. In the $\Xi^- \to \Lambda\pi^-, \Lambda \to p\pi^-$ process, the asymmetry parameters β and γ of the Ξ^- hyperon are accessible *via* the angular distribution of the protons [7]:

$$I(\theta_p, \phi_p) = \frac{1}{4\pi}(1 + \alpha_\Xi \alpha_\Lambda \cos\theta_p + \frac{\pi}{4}\alpha_\Lambda P_\Xi \sin\theta_p(\beta_\Xi \sin\phi_p - \gamma_\Xi \cos\phi_p)). \tag{3}$$

This is valid if the reference system is defined such that the spin of the Ξ^- hyperon is along the z-axis, the momentum of the daughter Λ hyperon is in the positive xz plane and the angles

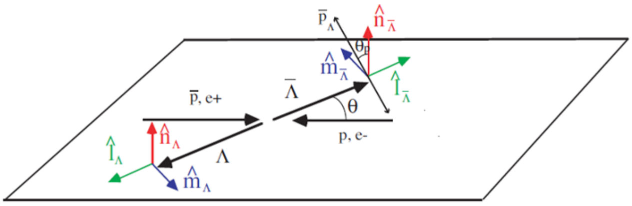

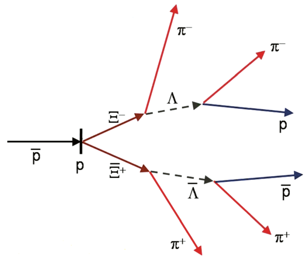

Figure 1. Left: Coord. system of $\overline{p}p \to \overline{Y}Y$. Right: The $\overline{p}p \to \overline{\Xi}\Xi, \Xi \to \Lambda\pi, \Lambda \to p\pi$ decay.

of the Ξ^- decay are integrated over. Furthermore, α_Λ is known, α_Ξ can be extracted from the angular distribution of the Λ from the Ξ^- decay and finally, $\alpha_\Xi^2 + \beta_\Xi^2 + \gamma_\Xi^2 = 1$ can be applied to extract all unknowns from Eq. 3.

Polarisation parameters for spin $\frac{3}{2}$ hyperons

For spin $\frac{3}{2}$ hyperons, the spin structure is more complicated. The L number in Eq. 1 can be 3, 2 or 1. This gives three Q_M^1, five Q_M^2 and seven Q_M^3 matrices, all in all fifteen Q_M^L matrices with fifteen corresponding r_M^L parameters. The spin density matrix was derived in Ref. [9]. Using symmetries imposed by strong interaction, eight polarisation parameters were found to be zero.

In the weak decay of a spin $\frac{3}{2}$ baryon into a spin $\frac{1}{2}$ baryon and a pseudoscalar, *e.g.* $\Omega \to \Lambda K^-$, the final state can have angular momentum $L = 1$, giving the parity conserving part of the decay matrix, or angular momentum $L = 2$, giving the parity violating part. It has been found that the asymmetry parameter α_Ω is consistent with zero [10] and in the following, it is set to exactly zero to simplify the calculations. Defining the reference system in the same way as in the spin $\frac{1}{2}$ case (see left panel of Fig. 1 but replace Λ with Ω and p with Λ) the angular distribution of the Λ from the Ω decay is given by

$$I(\theta_\Lambda, \phi_\Lambda) = \frac{1}{4\pi}(1 + \frac{\sqrt{3}}{2}(1 - 3\cos^2\theta_\Lambda)r_0^2 - \frac{3}{2}\sin^2\theta_\Lambda\cos 2\phi_\Lambda r_2^2 + \frac{3}{2}\sin 2\theta_\Lambda\cos\phi_\Lambda r_1^2) \tag{4}$$

Using the *method of moments* [8], the three polarisation parameters appearing in Eq. 4 can be obtained in terms of the moments of the sine and cosine functions, denoted within $\langle\rangle$:

$$\begin{aligned} r_0^2 &= \tfrac{15}{2\sqrt{3}}(\tfrac{1}{3} - \langle\cos^2\theta_\Lambda\rangle) \\ r_2^2 &= \tfrac{8}{3}(1 - \langle\cos^2\theta_\Lambda\rangle - 2\langle\sin^2\theta_\Lambda\sin^2\phi_\Lambda\rangle) \\ r_1^2 &= 5\langle\cos\theta_\Lambda\sin\theta_\Lambda\cos\phi_\Lambda\rangle \end{aligned} \tag{5}$$

For details, see Ref. [9]. More information about the remaining four non-zero polarisation parameters can be obtained by studying the combined angular distribution of the Λ hyperons from the Ω decay and the protons from the subsequent Λ decay, $I(\theta_\Lambda, \phi_\Lambda, \theta_p, \phi_p)$. The expression is lengthy for these proceedings but can be multiplied with certain trigonometric functions and integrated over the angles to extract the polarisation parameters [11]:

$$\begin{aligned} r_{-1}^1 &= -\frac{20\sqrt{10}\langle(3\cos\theta_\Lambda - 1)\sin\phi_p\rangle}{3\pi\alpha_\Lambda\gamma_\Omega} \\ r_{-1}^3 &= \frac{2\sqrt{5}\langle(15\cos\theta_\Lambda - 1)\sin\phi_p\rangle}{\sqrt{3}\pi\alpha_\Lambda\gamma_\Omega} \\ r_{-2}^3 &= -\frac{1024\langle\sin\phi_\Lambda\cos\phi_p\rangle}{3\pi^2\alpha_\Lambda\gamma_\Omega} \\ r_{-3}^3 &= -\frac{1}{5\sqrt{6}}(\frac{640}{\pi\alpha_\Lambda\gamma_\Omega}\langle\sin\phi_\Lambda\cos\phi_\Lambda\sin\phi_p\rangle + 4\sqrt{15}r_{-1}^3 + 3\sqrt{10}r_{-1}^1) \end{aligned} \tag{6}$$

Spin observables for $\frac{1}{2}$ hyperons in the $\overline{p}p \to \overline{Y}Y$ reaction

In the $\overline{p}p \to \overline{Y}Y$ reaction, not only the polarisation of individual hyperons are of interest, but also their correlations. In Ref. [12], the derivation of the spin observables for the spin $\frac{1}{2}$ case is performed in detail. Here we only summarise the results. The spin observables of the $\overline{p}p \to \overline{Y}Y$ reaction can be written in terms of the momentum vectors of the final state antibaryon $\overline{B}$ and baryon B from the $\overline{Y}$and Y decays:

$$I_0^{\overline{B}B} = \frac{I_0^{\overline{Y}Y}}{64\pi^3} \sum_{\mu,\nu=0}^{3} \sum_{i,j=0}^{3} \overline{\alpha}\alpha P_i^{\overline{p}} P_j^{p} \chi_{ij\mu\nu} \overline{k}_\mu k_\nu \tag{7}$$

where $I_0^{\overline{Y}Y}$ is the unpolarised angular distribution, α ($\overline{\alpha}$) denotes the asymmetry parameter of the Y ($\overline{Y}$), P_j^p ($P_i^{\overline{p}}$) the polarisation of the initial state proton (antiproton), k_ν ($\overline{k}_\mu$) the momentum vector of the final state decay baryon (antibaryon) and $\chi_{ij\mu\nu}$ the 256 spin observables. For the case of an unpolarised beam and an unpolarised target, $i = j = 0$, giving sixteen accessible variables. Due to symmetries, only six of these are non-zero: the polarisations $P_{\overline{Y},\mu} = \chi_{00\mu0}$ and $P_{Y,\nu} = \chi_{000\nu}$ and the spin correlations between the Y and the $\overline{Y}$, $C_{\mu\nu} = \chi_{00\mu\nu}$.

3. Prospects for PANDA

The foreseen PANDA experiment at FAIR opens up new possibilies in hyperon physics. The antiproton beam from the HESR storage ring, operating in an energy range between 1.5 GeV and 15 GeV, will interact with an internal hydrogen target. The PANDA experiment will have high luminosity and provide a near 4π acceptance featuring precise tracking and vertex reconstruction, sophisticated particle identification and calorimetry. For further details, see Ref. [13] and references therein. Simulation studies, described in Refs. [9, 16] show excellent prospects: high signal rate, low background rate and good detection efficiency over the full phase space for all single- and multi-strange and single-charmed hyperons. The estimated signal rates are given in Table 1. They are calculated assuming the high luminosity operating mode of the HESR that corresponds to $2{\cdot}10^{32}\text{cm}^{-2}\text{s}^{-1}$, as expected in the final version of FAIR. The only cross section that is well known here is the one for $\overline{p}p \to \overline{\Lambda}\Lambda$ at 1.64 GeV. In the remaining strangeness channels the quoted cross sections are extrapolations from data collected at other energies. For the Ω and Λ_c channels, no data exist. The quoted values of $\sigma(\overline{p}p \to \overline{\Omega}^+\Omega)$ and $\sigma(\overline{p}p \to \overline{\Lambda_c}\Lambda_c)$ are obtained from model calculations in Ref. [14] and [14, 15], respectively, and may be up to an order of magnitude different in reality. For the Λ and Ξ channels, the large foreseen statistics enables precision CP violation studies. If the cross section estimate for $\overline{p}p \to \overline{\Xi}^+\Xi^-$ is correct, the large Ξ data samples from HyperCP [17] can be exceeded in ≈80 days of data taking at 4 GeV. PANDA has the advantage that the $\overline{p}p$ in the initial state produces the same amount of hyperons and antihyperons. The simulation studies in Refs. [9, 16], show that spin observables of all hyperon channels can be well reconstructed in PANDA. Some examples are shown in Fig. 2.

4. Summary

The future PANDA experiment at FAIR has a unique opportunity to give new insights into the strong interaction in the confinement domain. Spin observables in antihyperon-hyperon production provide a powerful tool for this purpose. It will be possible to study the $\overline{p}p \to \overline{\Omega}^+\Omega^-$ reaction for the first time and seven non-zero polarisation parameters have recently been derived by the Uppsala group. Furthermore, high precision tests of CP violation in hyperon decay can be performed with the foreseen hyperon data samples from PANDA.

References

[1] Kohno M. and Weise W., 1986 *Phys. Lett.* B. **179** 15; Rubinstein H.R. and Snellman H. 1985 *Phys. Lett.* B. **165** 187; Furui S. and Faessler A. 1987 *Nucl. Phys.* A **486** 669;Burkardt M. and Dillig M. 1988 *Phys. Rev.* C **37** 1362; Alberg M.A. *et al.* 1988 *Z. Phys.* A **331** 207.

Table 1. Approximate foreseen production rates of various hyperon channels [9, 16]. The cross sections marked with a * have a very large uncertainty. Details are given in the text.

Beam mom. (GeV/c)	Reaction	σ (μb)	Eff (%)	Decay	Rate at $2{\cdot}10^{32}$cm^{-2}s^{-1}
1.64	$\overline{p}p \to \overline{\Lambda}\Lambda$	64	11	$\Lambda \to p\pi^-$	580 s^{-1}
4	$\overline{p}p \to \overline{\Lambda}\Lambda$	≈50	23	$\Lambda \to p\pi^-$	980 s^{-1}
15	$\overline{p}p \to \overline{\Lambda}\Lambda$	≈10	14	$\Lambda \to p\pi^-$	120 s^{-1}
4	$\overline{p}p \to \overline{\Lambda}\Sigma^0$	≈40	31	$\Sigma^0 \to \Lambda\gamma$	600 s^{-1}
4	$\overline{p}p \to \overline{\Xi}^+\Xi^-$	≈2	19	$\Xi^- \to \Lambda\pi^-$	30 s^{-1}
12	$\overline{p}p \to \overline{\Omega}^+\Omega^-$	≈0.002*	≈30	$\Omega \to \Lambda K^-$	≈80 h^{-1}
12	$\overline{p}p \to \overline{\Lambda_c}^-\Lambda_c^+$	≈0.1*	≈35	$\Lambda_c \to \Lambda\pi^+$	≈25 d^{-1}

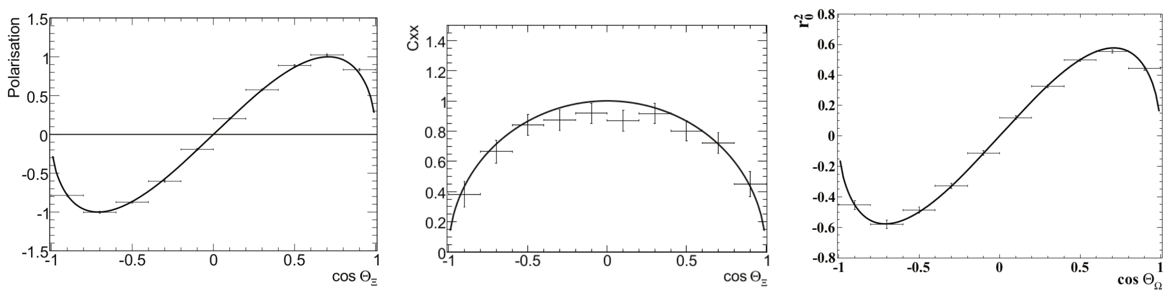

Figure 2. Left: The polarisation of the Ξ^- as a function of the Ξ^- scattering angle $\cos\theta_\Xi$. Middle: The spin correlation in the x direction (m in Fig. 1) of the $\overline{\Xi}^+$ and the Ξ^-. Right: The polarisation parameter r_0^2 of the Ω as a function of $\cos\theta_\Omega$. The points represent reconstructed values and the lines the input trigonometric functions.

[2] Tabakin F. and Eisenstein R.A. 1985 *Phys. Rev.* C **31** 1857; Kohno M. and Weise W., 1986 *Phys. Lett.* B. **179** 15; La France P. *et al.* 1988 *Phys. Lett.* B. **214** 317; Timmermans R.G.E. *et al.* 1992 *Phys. Rev.* D **45** 2288; Haidenbauer J. *et al.* 1992 *Phys. Rev.* C **46** 2516.
[3] Ortega P.G. *et al.* 2011 *Phys. Lett.* B. **696** 352.
[4] Sakharov A.D. 1967 *Pis'ma Zh. Eksp. Teor. Fiz.* **5** 32; Sakharov A.D. 1976 *JETP Lett.* **5** 24, [hep-ex/0408100].
[5] Doncel M.G. *et al.* 1972 *Nucl. Phys* B **38** 477; Doncel M.G. *et al.* 1973 *Phys. Rev.* D **7** 815.
[6] Pilkuhn H. 1967 *The interaction of hadrons* (North-Holland Publishing Company, Amsterdam)
[7] Koch W. 1968 *Analysis of scattering and decay* ed. Nikolic M. (Gordon and Breach, new York-London-Paris).
[8] Frodesen A.G. *et al.* 1979 *Probability and Statistics in Particle Physics* (Universitetsforlaget).
[9] Thomé E. 2012 *Multi-Strange and Charmed Antihyperon-Hyperon Physics for PANDA* Ph. D. Thesis, Uppsala University.
[10] Yao W. M. *et al.* [Particle Data Group] 2006 *J. Phys.* G **33** 1.
[11] Thomé E. 2013 *A Method for Measurement of Polarisation Parameters in the* $\overline{p}p \to \overline{\Omega}^+\Omega^-$ *Reaction* (in preparation).
[12] Paschke K. 2001 Ph. D. Thesis, Carnegie Mellon University.
[13] Fioravanti E. 2013 *Experimental overview of PANDA* (These proceedings).
[14] Kaidalov A.B. and Volkovitsky P.E. 1994 *Z. Phys.* C **63** 51
[15] Titov A.I. and Kämpfer B. 2008 *Phys. Rev.* C **78** 025201; Gornitschnig A.T. *et al.* 2009 *Eur. Phys. J.* A **42** 43; He J. *et al.* 2011 *Phys. Rev.* D **84** 114010; Khodjamirian A. *et al.* 2012 *Eur. Phys. J.* A **48**.
[16] Grape S. 2009 *Studies of PWO Crstals and Simulations of the* $\overline{p}p \to \overline{\Lambda}\Lambda, \overline{\Lambda}\Sigma^0$ *Reactions for the PANDA experiment* Ph.D. Thesis, Uppsala University.
[17] T. Holmstrom *et al.* 2004 *Phys. Rev. Lett.* **93** 262001.